Vibrational spectra of ammonia, benzene, and benzene adsorbed on Si (001) by *first principles* calculations with periodic boundary conditions

M. Preuss* and F. Bechstedt
Institut für Festkörpertheorie und -optik, Friedrich-Schiller-Universität, 07743 Jena, Germany
(Received 18 January 2006; revised manuscript received 6 March 2006; published 11 April 2006)

We develop an efficient method for the calculation of dynamical dipoles and frequencies of vibrational transitions in the framework of density-functional theory with periodic boundary conditions. It augments previous approaches by accounting for the substrate influence on the vibrations of the adsorbate. It allows one to reproduce and predict optical infrared and electron energy loss spectra including the correct relative oscillator strengths while still staying in the familiar picture of normal modes so that an intuitive physical interpretation of experimental results is possible.

DOI: 10.1103/PhysRevB.73.155413 PACS number(s): 78.30.−j, 68.35.Ja, 68.43.Pq

I. INTRODUCTION

Vibrational spectroscopy is one of the most powerful experimental techniques for the characterization of materials.[1,2] There is such a wealth of information on the spectroscopic properties of molecules and adsorbate complexes that, over the decades, a large database of wave numbers and eigenvectors of molecular vibrations has become available to researchers working in both chemistry and physics. The usefulness of these data lies in the fact that the vibrations can be classified according to a relatively simple scheme consisting of only a few number of characteristic types of vibrations—e.g., bending, stretching, rocking, and wagging modes—each of which have, depending on the species of the involved atoms, characteristic frequencies. Thus vibrational spectroscopy not only probes the symmetry and geometry of the atomic arrangement in question, but also, to a certain extent, the chemical composition. Thereby it provides insight into such complex issues as bonding mechanisms and adsorbate-substrate interactions.

The most prominent experimental techniques subsumed under the generic term "vibrational spectroscopy" are optical infrared (IR) spectroscopy, where light in the infrared region is shone on the sample, or high-resolution electron energy loss spectroscopy (HREELS), which probes the vibrations at the surface with a low-energy electron beam. The underlying physical process of IR spectroscopy is the coupling of the incident electric field to the dipoles accompanying the excitation of vibrational modes. This gives rise to resonant absorption peaks in dependence on the primary photon energy. In the case of normal incidence only in-plane dipoles are probed. Typical IR spectrometers are limited to an energy range between 10 and 1000 cm^{-1}, but provide an energy resolution of better than 1 cm^{-1}. HREEL spectroscopy exploits the effect of inelastic scattering of the incident electrons from the long-range dipole field above the crystal. The scattering is strongest in the forward direction.[3] Due to the grazing incidence geometry in which HREEL experiments are mainly carried out, this method dominantly probes vibrational dipoles perpendicular to the surface. HREELS covers a wider spectral range, but at the cost of a lower resolution of 10–30 cm^{-1}. Common to both kinds of spectroscopy is that excitations of vibrational modes are associated with vanishing or small momentum transfer so that zone-center optical modes can be observed, although larger phonon wave vectors may be studied by varying the scattering angle in the HREEL experiment. Both IR and HREELS are subject to the same selection rules[4] and can therefore conveniently be treated together.

Because of the complexity of either an IR or an HREEL spectrum the assignment of vibrational modes is usually not straightforward. However, knowledge of vibrational eigenfrequencies and eigenvalues from theory permits the interpretation of the peak structures of an experimental spectrum. This is where density-functional-theory (DFT) calculations have been proven helpful. The determination of vibrational frequencies within the harmonic approximation is a common task within the DFT method of calculating total energies for given atomic positions: Using advanced exchange-correlation functionals experimental wave numbers are usually reproduced within an error bar of less than 4%. The errors become larger the more complicated the involved vibrations are. The validity of the harmonic approximation may then become questionable due to strong anharmonic and long-range electric forces.

In addition to the frequencies the intensities of the vibrational transitions are crucial for the identification of characteristic features in a spectrum. These intensities are directly related to a dynamical dipole which corresponds to the change of the total dipole moment of the system as a response to a distortion along a certain normal mode. In DFT implementations using a localized basis set—e.g., GAUSSIAN[5]—the intensities of fundamental IR transitions are routinely calculated, but we are aware of only one paper[6] dealing with the calculation of parts of an HREEL spectrum within the framework of DFT with periodic boundary conditions.

The paper is organized as follows. Section II starts with a general overview of the used DFT implementation and proceeds with the details of the calculation of IR intensities. In Sec. III we present calculated IR spectra for the isolated molecules ammonia (NH_3) and benzene (C_6H_6) to test the reliability of our method. After that we show the calculated HREEL spectrum for the benzene-adsorbed Si (001) surface.

This system has been extensively studied experimentally during the last decades[7–12] and thus serves as an attractive benchmark for our method of calculation of vibrational spectra of complex systems. Section IV concludes with a summary.

II. COMPUTATIONAL METHODS

A. Total-energy calculations and modeling

The total-energy and electronic-structure calculations are performed using the Vienna *ab initio* simulation package (VASP) implementation[13] of the gradient-corrected (PW91) (Ref. 14) DFT. The electron-ion interaction is described within in the projecter-augmented wave (PAW) scheme pseudopotentials,[15,16] allowing for an accurate quantum-mechanical treatment of first-row elements with a relatively small basis set. We expand the electronic wave functions into plane waves up to an energy cutoff of 25 Ry, which has been demonstrated to be sufficient in previous studies on small organic molecules in the gas phase[17] and adsorbed on Si (001).[18,19]

Our calculations employ the residual minimization/direct inversion in the iterative subspace (RMM-DIIS) method [20,21] to minimize the total energy of the system. The molecular atomic structure is considered to be in equilibrium when the Hellmann–Feynman forces are smaller than 10 meV/Å. According to our tests this value is small enough to account for accurate forces and dipole moments. We apply artificial translational symmetries to describe both molecules in the gas phase and molecules adsorbed on solid substrates. The isolated molecules ammonia and benzene are arranged in cubic and hexagonal supercells, respectively, with edge lengths of 20 Å. Our test calculations have shown that this size is necessary to get rid of spurious interactions between the periodically repeated images of the molecules. The Si (001) surface with the 2×2 reconstruction is modeled with periodically repeated slabs where each supercell consists of six Si double layers plus adsorbed benzene molecules and a vacuum region equivalent in thickness to eight double layers. The corresponding slab bottom layer is hydrogen saturated and kept frozen during the structure optimization whereas all other atoms are allowed to relax. All surface calculations are performed with the calculated Si lattice constant of $a_{\mathrm{Si}}=5.470$ Å in an orthorhombic supercell with basis vectors $\boldsymbol{a}=a(\sqrt{2},0,0)$, $\boldsymbol{b}=a(0,\sqrt{2},0)$, and $\boldsymbol{c}=a(0,0,5)$. The Brillouin-zone integrations are carried out using only the Γ point in the case of isolated molecules and two $\boldsymbol{k}$ points in the irreducible part of the Brillouin zone in the case of surface calculations. For the determination of dipole moments a method introduced in Refs. 22 and 23 is used which essentially accounts for additional terms to the total energy for systems with a net dipole.

B. Calculation of eigenfrequencies and dynamical dipoles

A system with atoms in equilibrium positions responds to geometrical distortions with resulting forces which can be easily calculated by the Hellmann–Feynman theorem[24] as derivatives of the total energy with respect to (Cartesian) atomic coordinates. The linearization of these forces in the atomic displacements generates a $3N\times3N$ matrix (N is the number of atoms) called the Hessian or dynamical matrix of the system constructed as follows. Let $F_{\alpha\beta}^{\mu\nu,\pm}$ denote the νth Cartesian component of the resulting force on atom β due to a displacement of the αth atom in the positive (+) or negative (–) Cartesian direction μ. These forces build up the matrix $(K_{\alpha\beta}^{\mu\nu})$

$$K_{\alpha\beta}^{\mu\nu}=\frac{1}{2}\frac{F_{\alpha\beta}^{\mu\nu,+}-F_{\alpha\beta}^{\mu\nu,-}+F_{\beta\alpha}^{\nu\mu,+}-F_{\beta\alpha}^{\nu\mu,-}}{2d}, \tag{1}$$

which is symmetric with respect to a simultaneous change of α,β and μ,ν. The displacement d is to be chosen small enough to ensure harmonicity of the vibrations on the one hand and large enough to avoid numerical problems on the other. Empirically, values between 0.02 and 0.05 Å turn out to be well suited. In the end, of course, the result must be independent of the choice of d. The Hessian is defined as the quadratic matrix H with

$$H_{ij}\equiv H_{3(\alpha-1)+\mu,3(\beta-1)+\nu}=K_{\alpha\beta}^{\mu\nu}. \tag{2}$$

Obviously, as $1\leqslant\alpha,\beta\leqslant N$ and $1\leqslant\mu,\nu\leqslant3$, the indices of the Hessian cover the range $1\leqslant i,j\leqslant3N$. The generalized Newtonian equations of motion thus read

$$M\ddot{u}=-Hu, \tag{3}$$

with the matrix M of atomic masses,

$$M=\mathrm{diag}(m_1\mathbb{1}_3,m_2\mathbb{1}_3,\ldots,m_N\mathbb{1}_3),\quad \mathbb{1}_3=\mathrm{diag}(1,1,1), \tag{4}$$

and the displacement vector

$$u=(u_1,u_2,\ldots,u_{3N})^{\mathsf{T}}. \tag{5}$$

If a harmonic time dependence of the displacement vectors ($u=ze^{i\omega t}$) is assumed, the equations of motion reduce to the generalized eigenvalue problem

$$Hz=\omega^2Mz. \tag{6}$$

The resulting eigenvectors are M-orthogonal; i.e., the matrix $Z=(z_1,\ldots,z_{3N})$ of eigenvectors satisfies

$$Z^{\mathsf{T}}MZ=\mathbb{1}. \tag{7}$$

If the eigenvectors z_i, $i=1,\ldots,3N$, are scaled according to $q_i=M^{1/2}z_i$ where q_i is called normal coordinate, then the kinetic energy T and the potential energy V of the vibrating lattice are strictly quadratic in $\dot{q}_i$ and q_i, respectively:

$$T=\frac{1}{2}\sum_{i=1}^{3N}\dot{q}_i^2,\quad V=\frac{1}{2}\sum_{i=1}^{3N}\omega_i^2q_i^2. \tag{8}$$

By means of a basis change derivatives of a physical quantity A with respect to the normal coordinates can be expressed as derivatives with respect to Cartesian coordinates x_τ by

$$\frac{\partial A}{\partial q_i} = \sum_{\alpha=1}^{N} \sum_{\tau=1}^{3} \frac{\partial A}{\partial x_\tau} z_{i,3(\alpha-1)+\tau}, \quad i = 1, \ldots, 3N. \tag{9}$$

A central quantity derived from the changes of the system's dipole moment $\boldsymbol{\mu}$ with respect to the Cartesian coordinates of the αth atom is the *atomic polar tensor* (APT) $A^{(\alpha)}$, defined by its matrix elements as

$$A_{\nu\tau}^{(\alpha)} \equiv \frac{\partial \mu_\nu^{(\alpha)}}{\partial x_\tau}, \quad \nu, \tau = 1,2,3. \tag{10}$$

According to Wilson, Decius, and Cross,[25] the intensity of the ith normal mode in an infrared spectrum is given by

$$I_i \propto \left| \frac{\partial \boldsymbol{\mu}}{\partial q_i} \right|^2, \tag{11}$$

where we suppress any prefactors that depend on the measurement conditions because we are later mainly interested in relative intensities. By combining Eqs. (9) and (10) the relation between changes of the system's total dipole moment along the ith normal mode and the atomic polar tensors is established as

$$\frac{\partial \mu_\nu}{\partial q_i} = \sum_{\alpha=1}^{N} \sum_{\tau=1}^{3} \frac{\partial \mu_\nu^{(\alpha)}}{\partial x_\tau} z_{i,3(\alpha-1)+\tau} \tag{12a}$$

$$= \sum_{\alpha=1}^{N} \sum_{\tau=1}^{3} A_{\nu\tau}^{(\alpha)} z_{i,3(\alpha-1)+\tau}, \quad \nu = 1,2,3. \tag{12b}$$

The numerical implementation with a finite-difference approach to the calculation of changes of the dipole moment is straightforward within a central-difference scheme,

$$\frac{\partial \mu_\nu^{(\alpha)}}{\partial x_\tau} = \frac{\mu_\nu(x_\tau^{(\alpha)} + d) - \mu_\nu(x_\tau^{(\alpha)} - d)}{2d}, \tag{13}$$

where $\mu_\nu^{(\alpha)}$ indicates the νth component of the total dipole of the system that results from the displacement of the αth atom in the τth Cartesian direction.

There are three technical points to address. First, the construction of the full Hessian for N atoms within the central-difference scheme requires $2 \times 3N = 6N$ fully self-consistent calculations if no symmetry arguments help to reduce the computational cost. The demand in computing time can thus be high, depending on the system size. However, because the distortions from the equilibrium geometry are small, the electronic self-consistency cycle usually finishes after a few steps if it starts with the already converged electronic wave functions of the equilibrium configuration. As Eq. (13) is structurally the same as Eq. (1) the elements of the Hessian and dipole moment can be calculated accompanyingly. Second, especially in slab geometry, the number N of atoms chosen to include in the calculation determines to some extent the attainable range of the vibrational spectrum. If the adsorption of molecules on surfaces is studied, then the high-frequency region will be dominated by the adsorbate vibrations whereas the low-frequency part—say, below 300 cm^{-1}—is mostly the domain of lattice vibrations. If deeper-lying substrate atoms have to be included in the calculation, one will fall in the range of phonons where the validity of the above-mentioned method of calculation of intensities becomes questionable. The lattice dynamics is then more appropriately treated in the closely related so-called *ab initio* force constant method[26] or the density-functional perturbation theory[27] which allows for the calculation of the full phonon dispersion curves.

Third, in the case of vibrations of adsorbates at surfaces the *absolute* values of the calculated in-plane dipole moment components are less useful due to the periodic boundary conditions. Nevertheless, when related to a common point of reference, our test calculations have shown that the respective *changes* of these values can be used for the calculation of vibrational intensities in the same way as in the case for isolated molecules.

III. RESULTS AND DISCUSSION

A. Ammonia

Ammonia (NH_3) has been described and geometry-optimized in a $20 \times 20 \times 20$ Å^3 cubic unit cell with the three N-H bonds aligned parallel to the corner-to-corner diagonals of the cube. This arrangement results in identical N-H bond lengths of 1.020 Å and a H-N-H angle of 107.6°, both in close agreement with the values of 1.012 Å and 106.7° from Ref. 28. If the molecule, on the other hand, is aligned in such a way that the nitrogen lone pair orbital points in a direction parallel to one of the unit cell axes, the supercell arrangement breaks the C_{3v} symmetry of the isolated ammonia molecule by pushing one H atom 0.1 Å (0.05 Å) off the plane of the other two H atoms when put into a $10 \times 10 \times 10$ Å^3 ($20 \times 20 \times 20$ Å^3) supercell. We thus find a strong finite-size effect as an artifact of the supercell approximation that directly affects the geometry *and* the symmetry. This could be alleviated (theoretically) only by increasing the box size to infinity. The problem may become even more apparent when treating systems that are inherently incommensurate with any possible supercell—e.g., in the case of a structure with a fivefold symmetry which, of course, is not allowed in infinitely extended crystals. This is a critical point because the symmetry controls the (potential) degeneracies of vibrational and electronic states. If the symmetry is erroneously broken, also these degeneracies will be erroneously lifted. A further illustration of this problem can be found in Ref. 29.

Ammonia has a computed permanent dipole moment of 1.470 D, very close to the experimental value[28] of $\mu_{\text{expt}} = 1.471$ D. During the calculation of the IR intensities as described in Sec. II B with displacements of 0.05 Å in the positive and negative Cartesian directions it is changed by about 0.03 D. The C_{3v} group to which ammonia belongs consists of the identity operation E, two threefold rotation axes C_3, and three vertical mirror planes σ_v, in total three classes and therefore three irreducible representations. As each normal mode of vibration forms a basis for an irreducible representation of the point group of the molecule, the symmetry of the normal modes can be identified beforehand without knowing their shape. To this end it is convenient to determine the action of the symmetry elements of the respec-

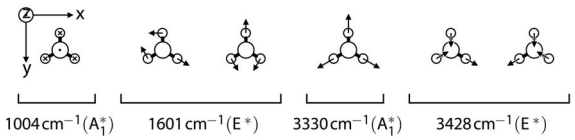

FIG. 1. Graphic representation of the normal modes of ammonia and their symmetry classification. N (H) atoms are shown as large (small) circles. The out-of-plane umbrella mode is depicted in such a way that atoms bearing dots (crosses) are displaced forwards (backwards). For the in-plane modes arrows (to scale for each mode) indicate atomic displacements in the paper plane. Infrared-active modes are labeled with an asterisk.

tive point group on the atoms constituting the molecule in a Cartesian basis. With a Cartesian coordinate system attached to each atom of the molecule, this leads to a (in general) reducible representation in the form of a $3N \times 3N$ matrix. The characters of these representation matrices under the symmetry operations of the point group C_{3v} read, for ammonia,

$$\Gamma_E = 12, \quad \Gamma_{C_3} = 0, \quad \Gamma_{\sigma_v} = 2. \tag{14}$$

Employing the standard notation of the C_{3v} character table,[30] this representation reduces to

$$\Gamma_{\text{tot}} = 3A_1 + A_2 + 4E. \tag{15}$$

As we are interested in pure vibrations only, we have to subtract the representations corresponding to pure translations and pure rotations. Doing this, we finally obtain

$$\Gamma_{\text{vib}} = 2A_1 + 2E. \tag{16}$$

Thus the six possible pure vibrations of the ammonia molecule belong to two one-dimensional and to two two-dimensional representations. Further inspection of the character table shows that all of them are symmetry-allowed—i.e., are IR active—and thus may also occur in an electron energy loss spectrum.

From the solution of the eigenvalue problem (6) of the vibrating lattice we not only obtain frequencies and mode intensities of a certain spectrum in an easy way, but also the displacement patterns of the normal coordinates. That means, above a quantitive analysis, we can also graphically describe the vibrations. The vibrational modes of ammonia are depicted in Fig. 1. They clearly reflect the symmetry of the C_{3v} point group. The symmetry classification according to the irreducible representations is done as follows: If a normal mode—say, q_i—belongs to a one-dimensional representation, any symmetry operation S of the group will carry q_i on itself or its negative self:

$$Sq_i = \pm q_i. \tag{17}$$

The symmetry operation can be expressed in a $3N \times 3N$ matrix (which already exists from the above determination of the symmetry species of the normal modes) and applied to the respective eigenvector. The resulting signs for S running through the symmetry operations are collected and compared to the character table. If, on the other hand, an eigenvalue—say, ω_k—is twofold degenerate, the corresponding eigenvectors q_{k1} and q_{k2} span a two-dimensional subspace in the eigenspace. Thus any symmetry operation S of the group applied to one of the q_{kj} will result in a linear combination of these two:

$$S\begin{pmatrix} q_{k1} \\ q_{k2} \end{pmatrix} = \begin{pmatrix} \alpha_1 & \beta_1 \\ \alpha_2 & \beta_2 \end{pmatrix}\begin{pmatrix} q_{k1} \\ q_{k2} \end{pmatrix}. \tag{18}$$

The traces of the coefficient matrices for S running through the symmetry elements are exactly the characters of the two-dimensional representation to which q_{k1} and q_{k2} belong. In other words, q_{k1} and q_{k2} together generate a certain representation or, put in a third way, q_{k1} and q_{k2} together transform according to the two-dimensional representation. This last mode of speaking becomes clear when looking at the E modes of ammonia: neither one nor the other vibration alone transforms according to the elements of the C_{3v} point group.

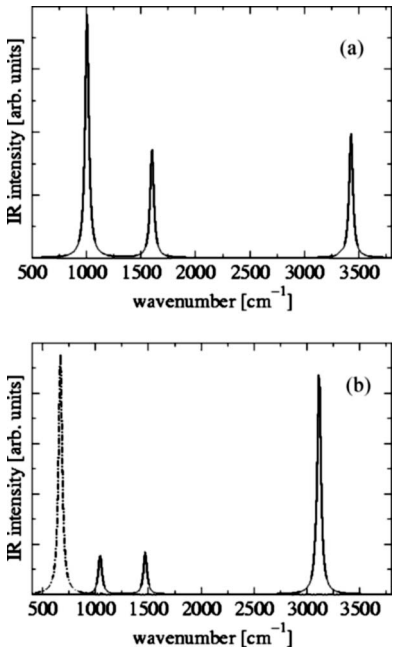

FIG. 2. Infrared spectrum of gas-phase (a) ammonia (NH_3) and (b) benzene (C_6H_6) calculated using the computed eigenfrequencies from Eq. (6) and the relative intensities from Eq. (11). For ammonia the total intensity contributions is drawn as a solid line; for benzene the in-plane (out-of-plane) intensity contribution is drawn as a solid (dash-dotted) line. A Lorentzian broadening of 20 cm^{-1} has been applied.

Due to the symmetry-induced degeneracy of the E vibrational modes, the spectrum in Fig. 2(a) consists of only four peaks of which, accidentally, the transition (in parentheses: experimental values from Ref. 31) at 3330 cm^{-1} (3337 cm^{-1}) has, though symmetry allowed as the corresponding normal mode belongs to the A_1 representation, a very low oscillator strength. The first peak at 1004 cm^{-1} (968 cm^{-1}) corresponds to the normal mode which may be pictorially imagined as the totally symmetric bending or "umbrella" mode, Fig. 1, and as such belongs to the totally symmetric A_1 representation. The second peak is due to the collective excitation of the normal modes belonging to the twofold-degenerate frequency of 1601 cm^{-1} (1628 cm^{-1}); the eigenvectors in the

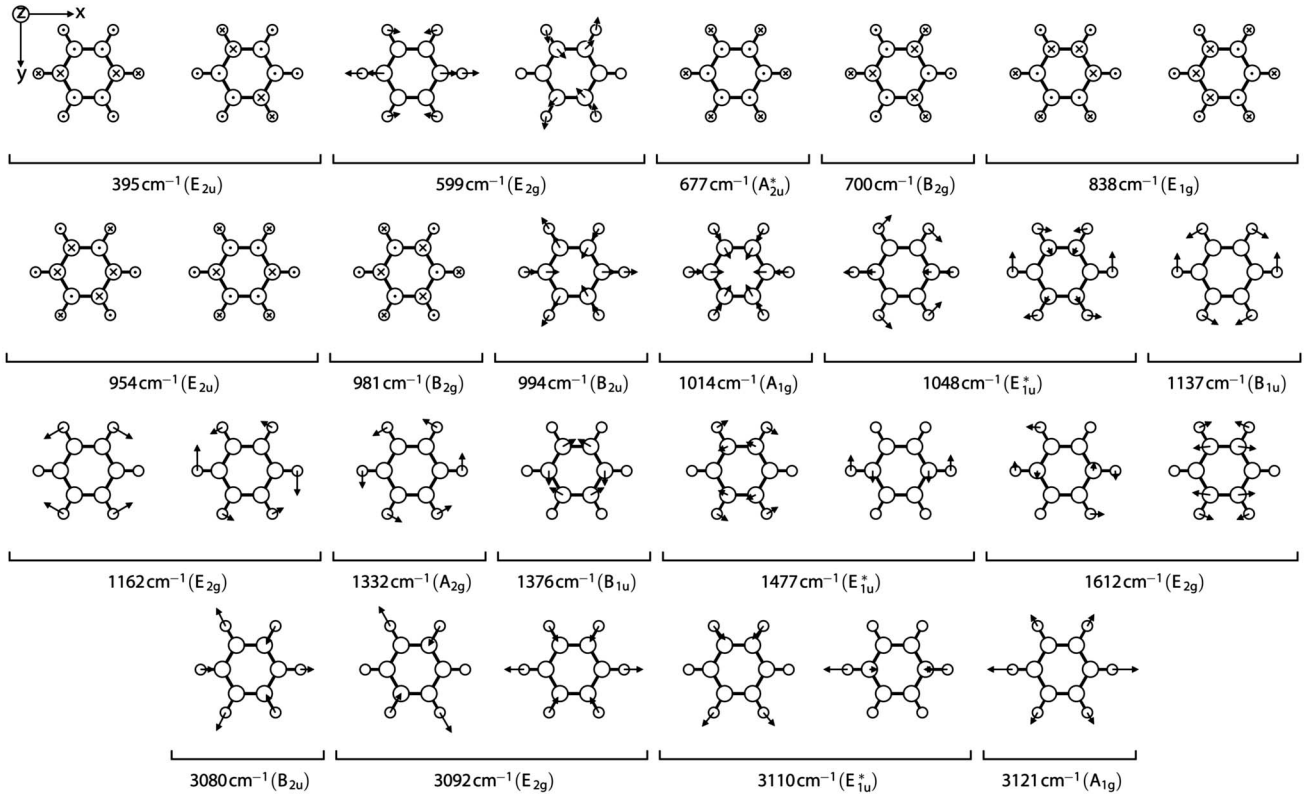

FIG. 3. Graphic representation of the normal modes of benzene and their symmetry classification. C (H) atoms are shown as large (small) circles. Out-of-plane modes are depicted in such a way that atoms bearing dots (crosses) are displaced forwards (backwards). For the in-plane modes arrows (to scale for each mode) indicate atomic displacements in the paper plane. Infrared-active modes are labeled with an asterisk.

corresponding subspace together transform according to the E representation. Each such an eigenmode consists of a bond stretching and a bond bending. The totally symmetric A_1 stretching mode at 3330 cm^{-1} does not show in the spectrum. The fourth peak is a result from the excitation of the two degenerate E eigenmodes with a frequency of 3428 cm^{-1} (3414 cm^{-1}), consisting of bond stretches and contractions. We state an excellent agreement between calculated and measured vibrational frequencies for ammonia: The spectral distance of the A_1 (E) modes is slightly underestimated (overestimated) by 1.8% (2.3%). The absolute differences vary between 3.7% for the lowest A_1 mode and 0.4% for the highest E modes.

B. Benzene

Benzene (C_6H_6) has been calculated and geometry-optimized using a hexagonal supercell with primitive basis vectors $\boldsymbol{a}=a(1,0,0)$, $\boldsymbol{b}=a(-1/2,\sqrt{3}/2,0)$, and $\boldsymbol{c}=(0,0,c)$ with $a=c=20$ Å. The molecule plane was aligned parallel to the $\boldsymbol{a}$-$\boldsymbol{b}$ plane and two C-C bonds parallel to the $\boldsymbol{a}$ and $\boldsymbol{b}$ axes. This arrangement results in C-C bond lengths of 1.398 Å and C-H bond lengths of 1.095 Å (experimental values from Ref. 28 are 1.399 and 1.101 Å, respectively). The correct D_{6h} symmetry demanded by the Kekulé structure is indeed determined by the internal symmetry analysis routine of the employed *ab initio* code VASP.

The vibrations of the benzene molecule can be classified according to the irreducible representations of the D_{6h} point group. Employing the above-mentioned strategy of determining the (reducible) representation in a Cartesian basis, reducing it, and omitting pure translational and pure rotational contributions, we end up with in total 30 vibrational modes,

$$\Gamma_{\text{vib}} = 2A_{1g} + A_{2g} + 2B_{2g} + E_{1g} + 4E_{2g} + A_{2u} + 2B_{1u} + 2B_{2u} + 3E_{1u} + 2E_{2u}. \quad (19)$$

All the vibrational modes of benzene are graphically represented in Fig. 3. This figure also indicates their symmetry classifications and the corresponding eigenfrequencies. Only those modes in Eq. (19) belonging to the A_{2u} or E_{1u} representation are IR active. These modes show up in the spectrum in Fig. 2(b): The A_{2u} out-of-plane mode (in parentheses: experimental values from Ref. 31) excited at 677 cm^{-1} (673 cm^{-1}) is indeed antisymmetric with respect to a C_2 axis perpendicular to the principal axis. The remaining three peaks in the spectrum at 1048 cm^{-1} (1038 cm^{-1}), 1477 cm^{-1} (1484 cm^{-1}), and 3110 cm^{-1} (3048 cm^{-1}) are due to excitations of normal modes which transform according to the E_{1u} representation of the D_{6h} point group.

The typical variation between the computed and measured eigenfrequencies amounts to 0.7%. Only for the highest allowed modes does this discrepancy slightly increase to 2%. Again we may state an excellent description of the vibra-

tional problem of the gas-phase benzene molecule within the developed supercell approach. Together with the good results obtained for other molecules, here shown for ammonia in Sec. III A, we suggest that the presented method should be also applicable to more complex systems—i.e., molecules adsorbed on solid substrates.

Here two remarks are appropriate concerning the method. First, of course numerical errors are inevitably introduced by the applied finite-difference approach to molecular motion. This leads to a small numerical lifting of degeneracies where the frequency differences between analytically degenerate modes increase the higher the vibrational energy becomes. The low-frequency E_{2u} modes at 395 cm^{-1}, e.g., are numerically degenerate within 1 cm^{-1} whereas the high-frequency E_{1u} modes at 3110 cm^{-1} are seemingly separated by 10 cm^{-1}. Despite this error, the symmetry analysis applied to the calculated normal-mode vectors indeed recovers all the irreducible representations noted in (19) correctly.

Second, due to the extremely high symmetry of the benzene molecule, the force constant matrix only has very few independent elements, so in principle it would suffice to displace one H and one C atom to obtain the full matrix with symmetry considerations. This could alleviate some of the numerical problems and may prove useful to save computational time in some cases, but it is restricted to high-symmetry systems. In the case of benzene on Si (001) we only find a C_1 symmetry for the total system. Nevertheless, we believe that a symmetry analysis of the adsorbed species (where applicable) alone treated as an isolated molecule is important to be better able to assess the changes that occur to the vibrations when adsorbed on the surface, with respect to the frequencies and to the intensities, but as well to the displacement patterns of the normal modes.

C. Benzene adsorbed on Si (001)

Various experimental and theoretical work[7–12] has been devoted to the adsorption of benzene on the Si (001) surface which emerged in the general agreement that benzene adsorbs in a butterfly fashion. Other suggested bonding geometries turned out instead to be either unstable or metastable. Thus we have started the structural optimization with a geometry such that the benzene (1,4) C atoms are aligned parallel to one Si dimer where we employed the asymmetrically buckled dimer model of the 2×2 reconstructed Si (001) surface. The resulting 1,4-cyclohexadiene-like butterfly geometry is depicted in Fig. 4. It is seen that because of the size of the benzene molecule, full monolayer coverage corresponds to one benzene molecule per 2×2 surface unit cell. So benzene relaxes from the planar gas-phase geometry with D_{6h} symmetry to a tilted cyclohexadiene structure with C_{2v} symmetry when adsorbed on Si (001). Despite this drastic reduction of symmetry it is still possible to uniquely relate the displacement patterns of the vibrations of the adsorbed species to those of the isolated benzene molecule.

Resulting from the interaction with the delocalized π-electron system of benzene, the buckling of the dimer with bonds to benzene vanishes whereas the buckling angle of the remaining Si dimer is essentially unchanged. This is in contrast to the cluster calculations done in Ref. 12 where the authors have *a priori* assumed a C_{2v} symmetry of the entire benzene/Si (001) adsorbate-substrate system. We find, though, that the buckling of the free dimer remains, but this does not affect the results because the vibration of the free Si dimer is a low-frequency lattice vibration that does not mix with the adsorbate-induced or adsorbate-dominated vibrations we are primarily interested in.

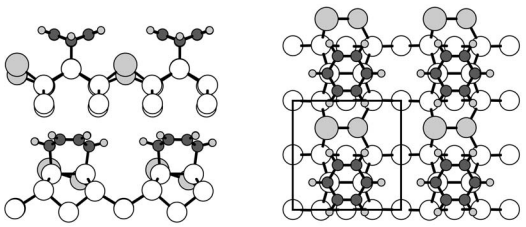

FIG. 4. Side views along the [011] and [0$\bar{1}$1] directions and top view of benzene adsorbed in a butterfly fashion on the Si (001) surface. Si atoms are sketched as large white circles, Si dimer atoms with no bonds to benzene as large gray circles; "up" and "down" dimer atoms are distinguished by size. Dark gray circles correspond to C atoms, small gray circles to H atoms. The 2×2 surface unit cell is indicated by a rectangle.

The calculated vibrational spectrum of benzene adsorbed on Si (001) is shown in Fig. 5. It is divided in out-of-plane (a) and in-plane (b) contributions. Here the term "out-of-plane" means the intensity resulting from the dynamical dipole perpendicular to the surface where "in-plane" corresponds to the components parallel to the surface. Obviously, the spectrum is much richer than that of the isolated benzene molecule because of the reduced symmetry and the interaction with the substrate. Nevertheless, it is possible to interpret the origin of most of the major peaks in terms of the vibrations of gas-phase benzene. To that end we compare the form and frequencies of the vibrations of the adsorbate-substrate system as depicted in Fig. 6 with the benzene modes as shown in Fig. 3. Afterwards we will identify common features in the calculated and measured HREEL spectrum.

We begin with the most important out-of-plane modes shown in Fig. 6(a). Although Si atoms are involved in the 295-cm^{-1} mode, the major displacements take place within the adsorbate which is found to correspond to one of the E_{2u} benzene modes with a frequency of 395 cm^{-1} (cf. Fig. 3). So this mode is softened by 100 cm^{-1} due to the interaction with the substrate. An additional feature seen in Fig. 6(a) for the 295-cm^{-1} mode is the symmetric up-and-down vibration of the Si dimer the benzene molecule is bonded to. The largest out-of-plane intensity peak at 757 cm^{-1} originates clearly from one of the E_{1g} modes at 838 cm^{-1}; the frequency shift of 81 cm^{-1} is related to the nearly complete immobilization of the two C atoms forming bonds to the surface Si dimer. The second largest peak at 3107 cm^{-1} results from the E_{1u} mode at 3110 cm^{-1} of benzene. It is shifted by merely 2 $cm^{-1}$and as such is characteristic for the adsorbate itself, in this case of a C-H stretch; the substrate influence is nearly neglegible.

The major in-plane modes and their coupling to the electromagnetic field or to electrons are characterized by the

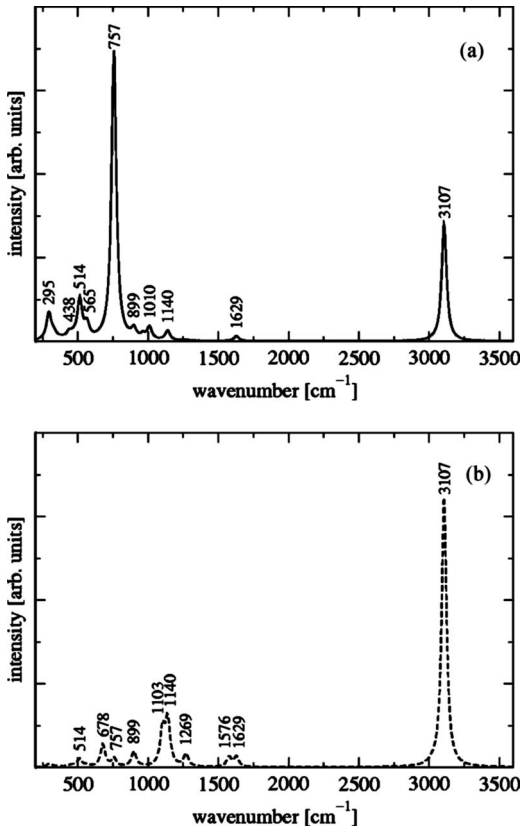

FIG. 5. IR spectrum of benzene adsorbed on Si (001). The solid line (a) represents the out-of-plane contributions, the dashed line (b) the in-plane contributions. Fundamental vibrations accompanied with a nonzero transition matrix element are referred to by their respective wave numbers (in cm^{-1}).

spectrum in Fig. 6(b). The peak at 1103 cm^{-1} is the result of the excitation of a B_{1u}-like normal mode of benzene at 1137 cm^{-1} which is redshifted by 36 cm^{-1} due to the molecule-substrate interaction. The 1140-cm^{-1} mode in the spectrum is due to one of the E_{2g} modes with a frequency of 1162 cm^{-1}. The mode with a frequency of 1332 cm^{-1} is partly similar to the A_{2g} benzene mode at 1333 cm^{-1}. A close look at the in-plane modes at 1576 and 1629 cm^{-1} shows that these two are most probably derived from the E_{2g} modes at 1612 cm^{-1}. While the symmetric C-C bond stretch at 1629 cm^{-1} is related directly to the E_{2g} mode, the asymmetric C-C bond stretch 1576 cm^{-1} obviously only becomes apparent when the molecule interacts with the surface. For a free molecule these two modes would be expected to vibrate with the same frequency—in other words, would be expected to be degenerate. The C-H stretch mode at 3107 cm^{-1} also shows up in the in-plane spectrum. All the observed redshifts and mode softenings may be simply explained by an increase of the "effective masses" of the atoms due to the presence of the heavier Si atoms.

Figure 7 demonstrates that our simple method of calculating frequencies and intensities of vibrational transitions yields a spectrum that for the major peaks compares very well to a measured HREEL spectrum of the adsorbate complex benzene on Si (001). We directly compare the frequencies of the adsorbate modes in Fig. 6 with the experimental

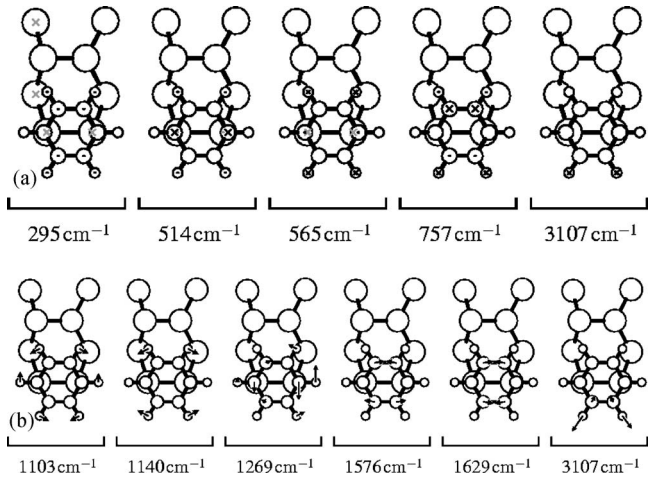

FIG. 6. Graphic representation of a selection of the IR- or HREELS-active (a) out-of-plane modes and (b) in-plane modes of vibration of benzene adsorbed on Si (001). C (H) atoms are shown as medium-sized (small) circles and Si atoms as large circles. The out-of-plane modes are depicted in such a way that atoms bearing dots (crosses) are displaced forwards (backwards). Gray dots and circles belong to distortions of substrate atoms. For the in-plane-modes the small arrows (to scale for each mode) indicate the displacements of the respective atoms.

ones from Fig. 7 (given in parentheses). The peak related to the C-H stretching vibration is reproduced at 3107 cm^{-1} (3050 cm^{-1}), but we fail to predict the smaller peak at 2935 cm^{-1} which Staufer *et al.*[12] attribute to the (1,4) C-H stretching—i.e., involving the C atoms bonded to the Si dimer. The measured double-peak structure may be traced back to a combination of the out-of-plane and in-plane modes in Fig. 6 with the highest frequencies. The peak at 1629 cm^{-1} (1623 cm^{-1}) results from the excitation of the normal mode involving the symmetric stretch of the remaining two C-C double bonds of the adsorbate. As discussed above, in the in-plane spectrum we find a mode involving the asymmetric stretch of the C-C double bonds which does not appear in the measured HREEL spectrum. The peak at 757 cm^{-1} (776 cm^{-1}) shows the highest relative intensity in the calculation as well as in the experimental spectrum; it is due to the excitation of an out-of-plane vibration of the C-C double bonds of opposite phase. We attribute the calcu-

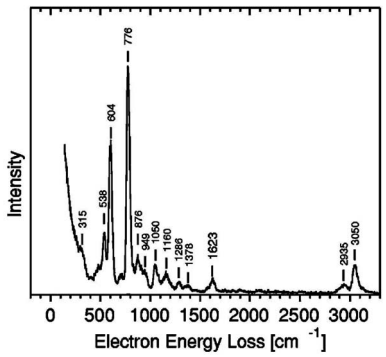

FIG. 7. Measured HREEL spectrum [modified version of the figure in Staufer *et al.* (Ref. 12)].

lated frequencies of 514 and 565 cm^{-1} to the experimental wave numbers 538 and 604 cm^{-1} because the displacement patterns of the corresponding normal modes are in accordance with the assignment of these modes by Staufer *et al.* Although the normal modes seem to be equivalent when looking at the projection on the surface plane, they differ considerably in amplitude. This becomes clear when keeping in mind that the mode with a frequency of 514 cm^{-1} leads to a nonvanishing contribution to the in-plane intensity as shown in Fig. 6(b) whereas the 565-cm^{-1} mode is forbidden in the in-plane spectrum. The first discernible experimental peak at 315 cm^{-1} we find to result from the excitation of the "butterfly-bending" normal mode with a calculated frequency of 295 cm^{-1} which we relate to the lowest-lying (395-cm^{-1}) fundamental mode of the isolated benzene molecule.

IV. SUMMARY

In this paper we presented a simple but accurate method for the calculation of the frequencies and oscillator strengths of vibrational transitions in systems with partial or full localization in the framework of density-functional theory with periodic boundary conditions. The method is suited for isolated molecules as well as for extended surface systems that can be described in a slab geometry. Together with the frequencies and displacement patterns of the calculated vibrations we are able to reproduce and predict IR and HREEL spectra including the correct relative intensities. Moreover, the results of these calculations also allow a qualitative interpretation in the intuitive graphical picture of normal modes. We have clearly demonstrated the influence of the actual adsorbate bonding and geometry on the vibrational spectra. Consequently, we expect the method to be helpful to unambiguously identify or discard suggested adsorption models by interpreting experimental IR and HREEL spectra. We have shown that the additional computational demand is relatively moderate and might even be reduced when exploiting potential symmetries of the adsorbate and/or the adsorbate complex.

ACKNOWLEDGMENTS

We thank the Deutsche Forschungsgemeinschaft for financial support (Grant No. SCHM-1361/6). We also acknowledge support from the EU network of Excellence NANOQUANTA (Grant No. NMP4-CT-2004-500198). Furthermore, we are indebted to Professor W. G. Schmidt, University of Paderborn, for inspiring this work. Grants of computer time from the Leibniz-Rechenzentrum München and the Höchstleistungs-Rechenzentrum Stuttgart are gratefully acknowledged.

*Electronic address: preuss@ifto.physik.uni-jena.de

[1] M. W. Urban, *Vibrational Spectroscopy of Molecules and Macromolecules on Surfaces* (Wiley, New York, 1994).
[2] H. Ibach and D. L. Mill, *Electron Energy Loss Spectroscopy and Surface Vibration* (Academic, New York, 1982).
[3] A. Zangwill, *Physics at Surfaces* (Cambridge University Press, Cambridge, UK, 1992).
[4] A. M. Bradshaw and N. V. Richardson, Pure Appl. Chem. **68**, 457 (1996).
[5] M. J. Frisch *et al.*, Computer Code GAUSSIAN 03, revision C.02, Gaussian, Inc., Wallingford, CT, 2004.
[6] Y. Morikawa, Phys. Rev. B **63**, 033405 (2001).
[7] G. P. Lopinski, D. J. Moffatt, and R. A. Wolkow, Chem. Phys. Lett. **282**, 305 (1998).
[8] U. Birkenheuer, U. Gutdeutsch, and N. Rösch, Surf. Sci. **409**, 213 (1998).
[9] M. J. Kong, A. V. Teplyakov, J. G. Lyubovitsky, and S. F. Bent, Surf. Sci. **411**, 286 (1998).
[10] K. Okamura, Y. Hosoi, Y. Kimura, H. Ishii, and M. Niwano, Appl. Surf. Sci. **237**, 439 (2004).
[11] K. W. Self, R. I. Pelzel, J. H. G. Owen, C. Yan, W. Widdra, and W. H. Weinberg, J. Vac. Sci. Technol. A **16**, 1031 (1998).
[12] M. Staufer, U. Birkenheuer, T. Belling, F. Nörtemann, N. Rösch, W. Widdra, K. L. Kostov, T. Moritz, and D. Menzel, J. Chem. Phys. **112**, 2498 (2000).
[13] G. Kresse and J. Furthmüller, Comput. Mater. Sci. **6**, 15 (1996).
[14] J. P. Perdew, J. A. Chevary, S. H. Vosko, K. A. Jackson, M. R. Pederson, D. J. Singh, and C. Fiolhais, Phys. Rev. B **46**, 6671 (1992).
[15] G. Kresse and D. Joubert, Phys. Rev. B **59**, 1758 (1998).
[16] P. E. Blöchl, Phys. Rev. B **50**, 17953 (1994).
[17] M. Preuss, W. G. Schmidt, K. Seino, J. Furthmüller, and F. Bechstedt, J. Comput. Chem. **25**, 112 (2004).
[18] K. Seino, W. G. Schmidt, M. Preuss, and F. Bechstedt, J. Phys. Chem. B **107**, 5031 (2003).
[19] M. Preuss, W. G. Schmidt, and F. Bechstedt, J. Phys. Chem. B **108**, 7809 (2004).
[20] P. Pulay, Chem. Phys. Lett. **73**, 393 (1980).
[21] D. M. Wood and A. Zunger, J. Phys. A **18**, 1343 (1985).
[22] G. Makov and M. C. Payne, Phys. Rev. B **51**, 4014 (1995).
[23] J. Neugebauer and M. Scheffler, Phys. Rev. B **46**, 16067 (1992).
[24] R. P. Feynman, Phys. Rev. **56**, 340 (1939).
[25] E. B. Wilson, J. C. Decius, and P. C. Cross, *Molecular Vibrations* (McGraw-Hill, New York, 1955).
[26] G. Kern, G. Kresse, and J. Hafner, Phys. Rev. B **59**, 8551 (1999).
[27] S. Baroni, S. de Gironcoli, A. D. Corso, and P. Giannozzi, Rev. Mod. Phys. **73**, 515 (2001).
[28] *Handbook of Chemistry and Physics*, 65th ed., edited by R. C. West (Chemical Rubber Company, Boca Raton, FL, 1984).
[29] P. H. Hahn, W. G. Schmidt, and F. Bechstedt, Phys. Rev. B **72**, 245425 (2005).
[30] F. A. Cotton, *Chemical Applications of Group Theory*, 3rd ed. (Wiley, New York, 1990).
[31] G. Herzberg, *Infrared and Raman Spectra of Polyatomic Molecules, Vol. 2 of Molecular Spectra and Molecular Structure* (van Nostrand, New York, 1959).